Inorg. Chem. **2008**, *47*, 3119−3127

Synthesis, Redox, and Amphiphilic Properties of Responsive Salycilaldimine-Copper(II) Soft Materials

Sarmad Sahiel Hindo,[†] Rajendra Shakya,[†] N. S. Rannulu,[†] Marco M. Allard,[†] Mary Jane Heeg,[†] M. T. Rodgers,[†] Sandro R. P. da Rocha,[‡] and Claudio N. Verani*[,†]

Department of Chemistry and Department of Chemical Engineering, Wayne State University, Detroit, Michigan 48202

Received November 13, 2007

Hydrolysis of the asymmetric pyridine- and phenol-containing ligand HL^1 (2-hydroxy-4-6-di-*tert*-butylbenzyl-2-pyridylmethyl)imine) led to the use of bis-(3,5-di-*tert*-butyl-2-phenolato-benzaldehyde)copper(II), $[Cu^{II}(L^{SAL})_2]$ (**1**) as a precursor for bis-(2,4-di-*tert*-butyl-6-octadecyliminomethyl-phenolato)copper(II), $[Cu^{II}(L^2)_2]$ (**3**), bis-(2,4-di-*tert*-butyl-6-octadecyl aminomethyl-phenolato)copper(II), $[Cu^{II}(L^{2A})_2]$ (**3′**), and bis-(2,4-di-*tert*-butyl-6-[(3,4,5-tris-dodecyloxy-phenylimino)-methyl]-phenolato)copper(II), $[Cu^{II}(L^3)_2]$ (**4**). These complexes exhibit hydrophilic copper-containing head groups, hydrophobic alkyl and alkoxo tails, and present potential as precursors for redox-responsive Langmuir–Blodgett films. All systems were characterized by means of elemental, spectrometric, spectroscopic, and electrochemical techniques, and their amphiphilic properties were probed by means of compression isotherms and Brewster angle microscopy. Good redox activity was observed for **3** with two phenoxyl radical processes between 0.5 and 0.8 V vs Fc^+/Fc, but this complex lacks amphiphilic behavior. To attain good balance between redox response and amphiphilicity, increased core flexibility in **3′** and incorporation of alkoxy chains in **4** were attempted. Film formation with collapse at 14 $mN \cdot m^{-1}$ was observed for the alkoxy-derivative but redox-response was seriously compromised. Core flexibility improved Langmuir film formation with a higher formal collapse and showed excellent cyclability of the ligand-based processes.

Introduction

Metal-containing soft materials merge the intrinsic properties of transition metals with those of functional organic scaffolds to build up organized architectures.[1,2] The relevance of such materials to the growing field of molecular electronics[3] is increasing considerably because it has been demonstrated that self-assembled films of triple-decker porphyrin-lanthanide precursors can be used for information storage.[4] In spite of the large footprint, these systems use multiple oxidations for writing of information, whereas the subsequent reductions are used for reading of stored data.[5]

Consequently, impending relevance can be envisioned for organized stimulus-responsive Langmuir–Blodgett films composed of monometallic precursors that present multiple redox states and smaller footprints. The stabilization of organic radicals in such precursors will play a vital role in attaining

* To whom correspondence should be addressed. E-mail: cnverani@chem.wayne.edu. Phone: 313 577 1076. Fax: 313 577 8022.
[†] Department of Chemistry.
[‡] Department of Chemical Engineering.

(1) (a) Bowers, J.; Amos, K. E.; Bruce, D. W.; Heenan, R. K. *Langmuir* **2005**, *21*, 5696. (b) Talham, D. R. *Chem. Rev.,* **2004**, *104*, 5479. (c) Griffiths, P. C.; Fallis, I. A.; Willock, D. J.; Paul, A.; Barrie, C. L.; Griffiths, P. M.; Williams, G. M.; King, S. M.; Heenan, R. K.; Görgl, R. *Chem.—Eur. J.* **2004**, *10*, 2022. (d) Rueff, J. M.; Masciocchi, N.; Rabu, P.; Sironi, A.; Skoulios, A. *Eur. J. Inorg. Chem.* **2001**, 2843.
(2) (a) Terazzi, E.; Suarez, S.; Torelli, S.; Nozary, H.; Imbert, D.; Mamula, O.; Rivera, J.-P.; Guillet, E.; Bénech, J.-M.; Bernardinelli, G.; Scopelliti, R.; Donnio, B.; Guillon, D.; Bünzli, J.-C.; Piguet, C. *Adv. Funct. Mater.* **2006**, *16*, 157. (b) Serrano, J. L.; Sierra, T. *Coord. Chem. Rev.* **2003**, *242*, 73. (c) Donnio, B. *Curr. Opin. Colloid Interface Sci.* **2002**, *07*, 371.
(3) (a) Low, P. J. *Dalton Trans.* **2005**, 2821. , and references therein. (b) Joachin, C.; Gimzewski, J. K.; Aviran, A. *Nature* **2000**, *408*, 541. (c) Dei, A.; Gatteschi, D.; Sangregorio, C.; Sorace, L. *Acc. Chem. Res.* **2004**, *37*, 827. (d) Kahn, O.; Martinez, C. J. *Science* **1998**, *279*, 44. (e) Verdaguer, M. *Science* **1996**, *272*, 698.
(4) Liu, Z.; Yasseri, A. A.; Lindsey, J. S.; Bocian, D. F. *Science* **2003**, *302*, 1543.
(5) (a) Padmaja, K; Youngblood, W. J.; Wei, L.; Bocian, D. F.; Lindsey, J. S. *Inorg. Chem.* **2006**, *45*, 5479. (b) Roth, K. M.; Dontha, N.; Dabke, R. B.; Gryko, D. T.; Clausen, C.; Lindsey, J. S.; Bocian, D. F.; Kuhr, W. G. *J. Vac. Sci. Technol.* **2000**, *18B*, 2359.
(6) (a) Lanznaster, M.; Hratchian, H. P.; Heeg, M. J.; Hryhorczuk, L. M.; McGarvey, B. R.; Schlegel, H. B.; Verani, C. N. *Inorg. Chem.* **2006**, *45*, 955. (b) Lanznaster, M.; Heeg, M. J.; Yee, G. T.; McGarvey, B. R.; Verani, C. N. *Inorg. Chem.* **2007**, *46*, 72.

10.1021/ic702233n CCC: $40.75
Published on Web 03/13/2008

redox states beyond those expected for the metallic ion. Ligands based on *tert*-butyl substituted phenolates[6,7] ensure the required phenolate/phenoxyl bistability[8] needed to render their complexes as viable prototypical molecular switches that enable multiple read/write cycles.

Copper(II) salicylaldehydes have been used as synthetic precursors in the self-assembly of catalysts,[9,10] in smectic mesogens to avoid bimetallic cores,[11] as well as in modified electrodes.[12] The seminal work of Nagel et al.,[13] entailing the condensation of hexadecylamine with 4-hydroxysalicylaldehyde applied this concept to metallosurfactants while pointing to the importance of polar substituents attached to the headgroup to achieve organized monolayers. Therefore, the main challenge in the development of precursors based on *tert*-butyl substituted phenolates is the fact that while these groups can enhance the redox properties, their bulkiness and apolar nature may compromise the amphiphilic behavior of the resulting materials.

We have developed and studied iron(III)- and cobalt(II/III)-containing soft materials based on the asymmetric pyridine and phenol pendant-arms ligand HL^1, depicted in its deprotonated form in Scheme 1.[14] Owing to this interest, the synthesis and characterization of copper(II) complexes was attempted, but ligand hydrolysis yielded $[Cu^{II}(L^{SAL})_2]$ (**1**) where L^{SAL-} is the deprotonated 2,4-*tert*-butylsalycilaldehyde as the main product and $[(L^{SAL})_2Cu^{II}_2(\mu\text{-}OCH_3)_2]$ (**5**) as a minor component. Because free copper(II) ions mediate ligand hydrolysis,[15] **1** was used as a precursor for the formation of $[Cu^{II}(L^1)_2]$ (**2**), as well as for the metallosurfactants $[Cu^{II}(L^2)_2]$ (**3**) and $[Cu^{II}(L^3)_2]$ (**4**). Complex **3** allows for in situ reduction yielding the equivalent and more flexible amine complex $[Cu^{II}(L^{2A})_2]$ (**3′**). Species **3**, **3′**, and **4** are candidates as amphiphilic precursors for redox-responsive Langmuir–Blodgett films. This paper describes the delicate balance between redox and amphiphilic behavior observed in these species and offers a rationale for improving these properties, the advantages, and the limitations of this approach. These findings are expected to have a positive impact in the future design of responsive films.

Scheme 1. Complexes and Their *tert*-Butyl Substituted Ligands

The Complexes:

$[Cu^{II}(L^{SAL})_2]$	(1)	$[Cu^{II}(L^{2A})_2]$	(3')
$[Cu^{II}(L^1)_2]$	(2)	$[Cu^{II}(L^3)_2]$	(4)
$[Cu^{II}(L^2)_2]$	(3)	$[(L^{SAL})_2Cu^{II}_2(\mu OCH_3)_2]$	(5)

The Ligands:

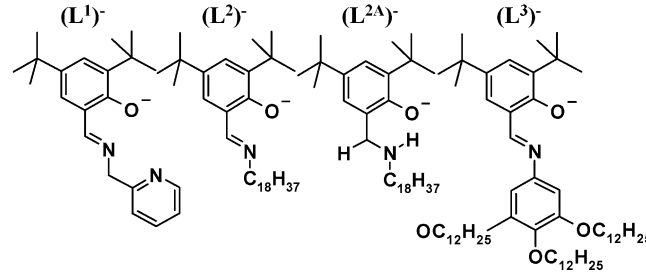

Results and Discussion

Ligand Hydrolysis. Treatment of HL^1 with hydrated copper(II) perchlorate in methanol produced $[Cu^{II}(L^1)_2]$ (**2**) in poor yields. The electrospray ionization (ESI) mass spectrum (positive ion mode) of the isolated compound presented $m/z = 710$ for $[\mathbf{2} + H^+]^+$. However, the spectrum of the reaction mixture contained peaks at $m/z = 530$ and 655 suggesting the presence of additional products along with **2**. In wet methanol, the peak at $m/z = 530$ became dominant and was identified as related to the main hydrolysis product $[Cu^{II}(L^{SAL})_2]$ (**1**) as $[\mathbf{1} + H^+]^+$. Slow evaporation of the solvent yielded a few crystals of $[(L^{SAL})_2Cu^{II}_2(\mu CH_3O)_2]$ (**5**) that presented $m/z = 655$ for $[\mathbf{5} + H^+]^+$. Infrared spectroscopy of the isolated solids revealed strong peaks at 1619 and 1424 cm^{-1}, attributed to the stretching and bending modes of carbonyl groups, respectively. Precursor **1** was later obtained synthetically in gram amounts and yielded X-ray quality crystals.

X-ray Structures. Both **1** and **5** were analyzed by single crystal diffraction methods and their molecular structures are displayed in Figure 1. Complex **1** shows two deprotonated ligands coordinated to a copper(II) center in a square-planar environment where the O−Cu−O angles deviate slightly from the expected 90.0°. The ligands are positioned trans to one another, and the molecule adopts an approximate D_{2h} local symmetry. The bond lengths of the $Cu-O_4$ coordination sphere are in good agreement with similar species reported in the literature,[16] where the $Cu-O_{carbonyl}$ bonds are longer than the $Cu-O_{phenolate}$ bonds. The entire molecule minus the *tert*-butyl substituents is planar (mean deviation 0.02 Å). There are no close axial contacts nor ligands to Cu and no

(7) (a) Philibert, A.; Thomas, F.; Philouze, C.; Hamman, S.; Saint-Aman, E.; Pierre, J. L. *Chem.—Eur. J.* **2003**, *09*, 3803. (b) Thomas, F.; Gellon, G.; Gautier-Luneau, I.; Saint-Aman, E.; Pierre, J.-L. *Angew. Chem., Int. Ed.* **2002**, *41*, 3047. (c) Shimazaki, Y.; Huth, S.; Odani, A.; Yamauchi, O. *Angew. Chem., Int. Ed.* **2000**, *39*, 1666. (d) Jazdzewski, B. A.; Tolman, W. B. *Coord. Chem. Rev.* **2000**, *200*(202), 633. (f) Hockertz, J.; Steenken, S.; Wieghardt, K.; Hildebrandt, P. *J. Am. Chem. Soc.,* **1993**, *115*, 11222.

(8) (a) Marchivie, M.; Guionneau, P.; Howard, J.; Chastanet, G.; Letard, J.-F.; Goeta, A.; Chasseau, D. *J. Am. Chem. Soc.* **2002**, *124*, 194. (b) Pease, A. R.; Jeppesen, J. O.; Stoddart, J. F.; Luo, Y.; Collier, C. P.; Heath, J. R. *Acc. Chem. Res.* **2001**, *34*, 433. (c) Fabbrizzi, L.; Licchelli, M.; Pallavicini, P. *Acc. Chem. Res.* **1999**, *32*, 846.

(9) Murphy, E. F.; Schmid, L.; Bürgi, T.; Maciejewski, M.; Baiker, A. *Chem. Mater.* **2001**, *13*, 1296.

(10) Murphy, E. F.; Ferri, D.; Baiker, A. *Inorg. Chem.* **2003**, *42*, 2559.

(11) Paschke, R.; Liebsch, S.; Tschierske, C.; Oakley, M. A.; Sinn, E. *Inorg. Chem.* **2003**, *42*, 8230.

(12) Shervedani, R. K.; Mozaffari, S. A. *Anal. Chem.* **2006**, *78*, 4957.

(13) Nagel, J.; Oertel, U.; Friedel, P.; Komber, H.; Möbius, D. *Langmuir* **1997**, *13*, 4693.

(14) (a) Shakya, R.; Hindo, S. S.; Wu, L.; Allard, M.; Heeg, M. J.; Hratchian, H. P.; McGarvey, B. R.; da Rocha, S.; Verani, C. N. *Inorg. Chem.* **2007**, *46*, 9808. (b) Shakya, R.; Imbert, C.; Hratchian, H. P.; Lanznaster, M.; Heeg, M. J.; McGarvey, B. R.; Allard, M.; Schlegel, H. B.; Verani, C. N. *Dalton Trans.* **2006**, 2517. (c) Imbert, C.; Hratchian, H. P.; Lanznaster, M.; Heeg, M. J.; Hryhorczuk, L. M.; McGarvey, B. R.; Schlegel, H. B.; Verani, C. N. *Inorg. Chem.* **2005**, *44*, 7414.

(15) (a) Eichhorn, G. L.; Bailar, J. C., Jr. *J. Am. Chem. Soc.,* **1953**, *75*, 2905. (b) Eichhorn, G. L.; Marchand, N. D. *J. Am. Chem. Soc.,* **1956**, *78*, 2688.

(16) (a) Lin, Z.-D.; Zang, W. *Acta Crystallogr.* **2006**, *E62*, 1074. (b) Sun, Y.-X.; Gao, G.-Z. *Acta Crystallogr.* **2005**, *E61*, 354. (c) Ali, H. M.; Abdul Halim, S. N.; Ng, S. W. *Acta Crystallogr.* **2005**, *E61*, 1429. (d) Elmali, A.; Elerman, Y.; Svoboda, I.; Fuess, H. *Z. Kristallogr.* **1995**, *210*, 612.

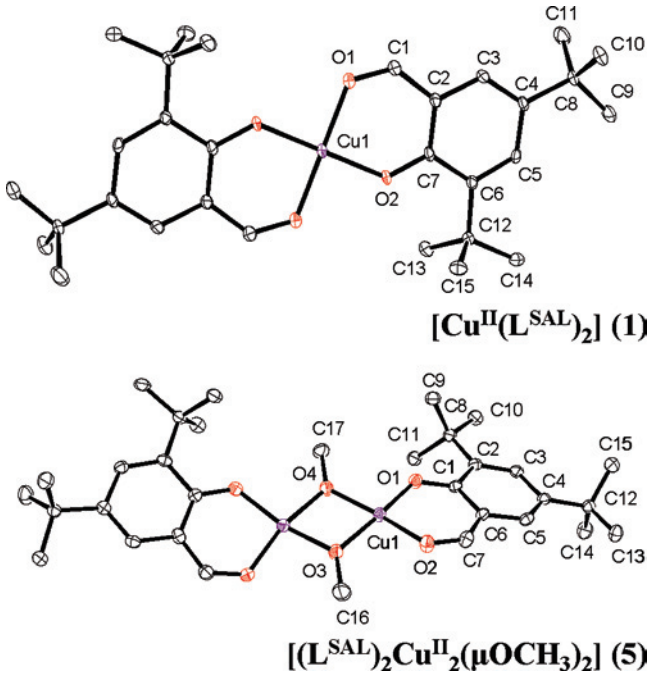

Figure 1. ORTEP diagrams for **1** and **5**. Selected bond lengths (Å) and angles (°) for **1**: Cu(1)−O(2) = 1.876; Cu(1)−O(1) = 1.952; C(1)−O(1) = 1.254; C(7)−O(2) = 1.305, O(2)−Cu(1)−O(2) = 180.00; O(1)−Cu(1)−O(1) = 180.00; O(2)−Cu(1)−O(1) = 92.83; O(2)−Cu(1)−O(1) = 87.17. For **5**: Cu(1)−Cu(1) = 2.996; Cu(1)−O(1) = 1.894; Cu(1)−O(3) = 1.895; Cu(1)−O(4) = 1.914; Cu(1)−O(2) = 1.933; C(1)−O(1) = 1.301; C(7)−O(2) = 1.253; Cu(1)−O(4)−Cu(1) = 103.02; O(3)−Cu(1)−O(4) = 76.25; O(1)−Cu(1)−O(3) = 167.51; O(4)−Cu(1)−O(2) = 166.41; O(1)−Cu(1)−O(4) = 96.80; O(1)−Cu(1)−O(2) = 94.40; O(3)−Cu(1)−O(2) = 94.03.

ring stacking nor counterions are present. The binuclear complex **5** shows two copper(II) ions doubly bridged by two deprotonated methoxide groups. Each copper center is also coordinated to a 3,5-di-*tert*-butyl-2-hydroxybenzaldehyde ligand in distorted square planar geometries. Interestingly, the molecule presents idealized C_{2v} symmetry with the two ligands positioned cis to one another, thus suggesting that dimer formation may precede hydrolysis. Bond lengths and angles are in good agreement with similar structures.[17] Because few crystals of this dimer were generated, no further investigations were carried out.

Syntheses. The formation of **1** as the main product of imine hydrolysis has driven a series of reactivity studies in which several amine-containing substrates were tested. When **1** was treated with 2-aminomethylpyridine, the initially targeted **2** was obtained, as indicated by the peak at m/z = 710 in the ESI mass spectrum corresponding to $[\mathbf{2} + H^+]^+$ with the proper isotopic distribution. When 2-aminomethylpyridine was replaced by 1-octadecylamine and 1,2,3-tris(dodecyloxy)-5-methylbenzene, the amphiphiles **3** and **4** were obtained as shown in Scheme 2. These species were isolated and carefully investigated by several spectroscopic methods. The most remarkable feature in the infrared spectrum of **1** is associated with the stretch of the carbonyl groups ($\nu_{C=O}$) at 1619 cm^{-1}. This peak disappears for **2**, **3**, and **4** and a new peak is observed around 1588 cm^{-1} for the

Scheme 2. Structures for **3**, **3′**, and **4** and Their ESI(Pos) Peak Clusters for $[M + H^+]^+$ [a]

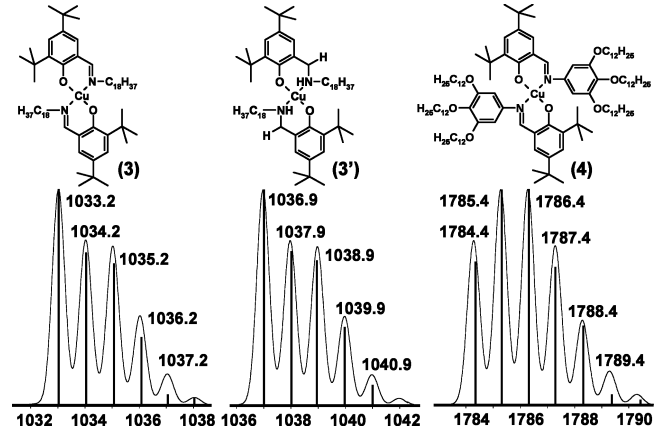

[a] The relative abundance axis of each complex is omitted for clarity.

C=N stretch of imine groups. The absence of strong peaks around 1090 cm^{-1} for all isolated complexes indicates lack of perchlorate counterions and supports the presence of two coordinated phenolates in a neutral molecule. To test the effect of a decreased framework rigidity, reduction of the imine −C=N− bonds was attempted by treating **3** and **4** with sodium borohydride and aiming at the equivalent but more flexible amine −HC−NH− counterparts. These attempts failed for **4** but worked well for the octadecylamine-substituted ligand in **3** converting it to **3′** in quantitave yields. The identity of the compound was confirmed by infrared spectroscopy and mass spectrometry: disappearance of the C=N stretch peak along with a corresponding 4 mass-unit increase, related to the addition of two hydrogen atoms per ligand, was observed. The elemental analyses of **3**, **3′**, and **4** are in excellent agreement with these formulations. block

Electronic Spectra. The electronic spectra of **1**, **3**, and **4** were measured in dichloromethane as a characterization tool for the new amphiphiles. Figure 2 displays intense bands observed in the ultraviolet and early visible range, whereas much less intense d−d bands (not shown) are observed between 600 and 1000 nm. The bands around 250–280 and 310–325 nm are attributed to intraligand $\sigma \rightarrow \pi^*$ and/or $\pi \rightarrow \pi^*$ transitions. The nature of the bands in the 380–420 nm range has been previously assigned to intraligand processes, metal-to-ligand, and ligand-to-metal charge transfers.[18–21] These bands are assigned as having a predominant ligand-to-metal charge transfer character. The presence of $N_{imine} \rightarrow Cu^{II}$ and $O_{phenolate} \rightarrow Cu^{II}$ charge transfers is suggested because of the presence of high extinction coefficients.

(17) Wrobleski, D. A; Rauchfuss, T. B.; Rheingold, A. L.; Lewis, K. A. *Inorg. Chem.* **1984**, *23*, 3124.

(18) (a) Rigamonti, L.; Demartin, F.; Forni, A.; Righetto, S.; Pasini, A. *Inorg. Chem.* **2006**, *45*, 10976. (b) Iglesias, A. L.; Aguirre, G.; Somanathan, R.; Parra-Hake, M. *Polyhedron* **2004**, *23*, 3051.

(19) (a) Kasumov, V. T.; Koeksal, F.; Sezer, A. *Polyhedron* **2005**, *24*, 1203. (b) Kuzniarska-Biernacka, I.; Kurzak, K.; Kurzak, B.; Jezierska, J. *J. Sol. Chem.* **2003**, *32*, 719. (c) Losada, J.; del Peso, I.; Beyer, L. *Inorg. Chim. Acta* **2001**, *321*, 107. (d) Kurzak, K.; Kuzniarska-Biernacka, I.; Kurzak, B.; Jezierska, J. *J. Sol. Chem.* **2001**, *30*, 709.

(20) (a) Bill, E.; Müller, J.; Weyhermüller, T.; Wieghardt, K. *Inorg. Chem.* **1999**, *38*, 5795. (b) Auerbach, U.; Eckert, U.; Wieghardt, K.; Nuber, B.; Weiss, J. *Inorg. Chem.* **1990**, *29*, 938.

(21) (a) Jazdzewski, B. A.; Holland, P. L.; Pink, M.; Young, V. G., Jr.; Spencer, D. J. E.; Tolman, W. B. *Inorg. Chem.* **2001**, *40*, 6097.

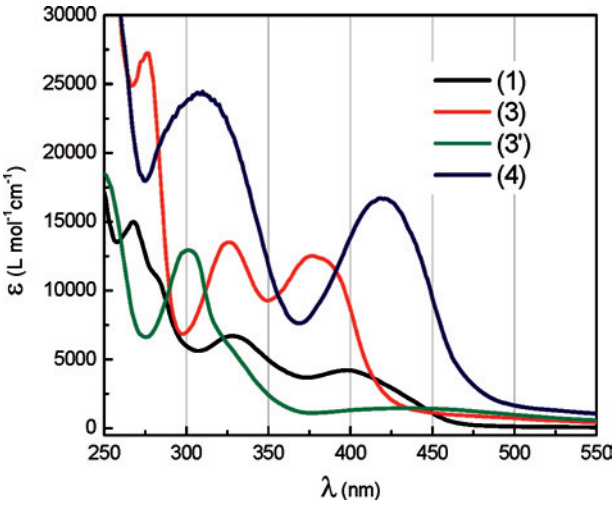

Figure 2. UV–visible spectra for **1**, **3**, **3′**, and **4** in 1.0×10^{-4} M dichloromethane solutions. λ_{max}, nm (ε, $L \cdot mol^{-1} \cdot cm^{-1}$) for **1**: 282 (15,600), 325 (9500), 403 (7700); for **3** 276 (27,200), 325 (13,300), 380 (12,500); for **3′** 229 (18,300), 301 (13,100), 330sh (∼4000), 448 (1900); for **4** 250 (∼39,000), 310 (24,500), 420 (16,700). The d−d bands are found at 692 (170) for **1**, 662 (260) for **3**, 680 (280) for **3′**, and 725 (350) for **4**.

The position of this band in **3** is in good agreement with other alkyl-substituted ligands in similar solvents,[22] but its intensity is considerably decreased in **3′** where the aldimine chromophore has been reduced. Also noteworthy is the fact that when comparing **1** and **3**, a hypsochromic (blue) shift of ∼20 nm is observed, but comparison between **1** and **4** reveals a ∼20 nm bathochromic (red) shift. Because all of these species have tertiary butyl groups attached to the second and fourth positions of the phenolate rings, the nature of the groups in the sixth position must be considered, namely carbaldehyde for **1**, octadecyliminomethyl for **3** and **3′**, and tris(dodecyloxy)phenyl-iminomethyl for **4.** Assuming some degree of distortion from square planar to tetrahedral[23] in **3** and **4**, the hypsochromic effect is attributed to the free motion of these alkyl groups that leads to distortions on the iminomethyl moiety diminishing the extent of the π-delocalization. The bulky nature of the phenyl groups in **4**, as well as the presence of the trialkoxy auxochromes, is suggested to stabilize π-delocalization.

Redox Properties. Cyclic voltammograms in dichloromethane solutions of **1**, **3**, **3′**, and **4** were measured to assess the redox potentials of ligand-centered processes. All potentials are reported at 100 $mV \cdot s^{-1}$ and versus the Fc^+/Fc couple, unless noted otherwise. A study was also performed to evaluate the reversibility of the phenolate/phenoxyl couples in **3** and **3′** by cycling 50 times through the wave associated with the first and second ligand-centered process. This cycling is intended to simulate switching mechanisms that will play a key role in responsive films. These results are shown in Figure 3. For all compounds the metal-centered reduction is observed between −1.60 and −1.80 V, whereas the oxidation appears around −0.90 and −1.20 V. All processes are irreversible with peak separations (ΔEp)

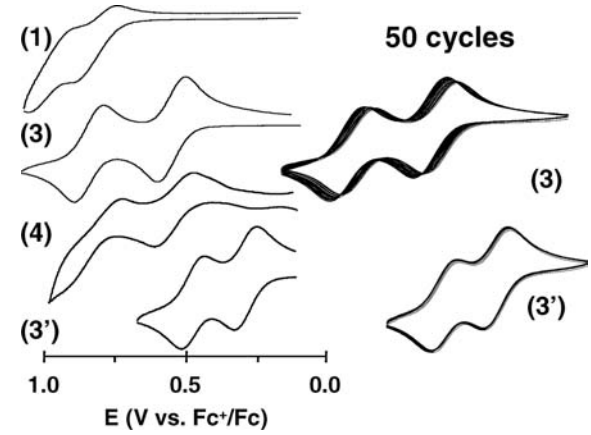

Figure 3. Cyclic voltammetry of 1.0×10^{-3} M CH_2Cl_2 solutions of **1**, **3**, **3′**, and **4**: First and second ligand-centered processes at 0.82 and 0.98 for **1**; 0.54 and 0.83 for **3**; 0.29 and 0.48 for **3′**; and 0.53 and 0.80 V vs Fc^+/Fc for **4**. The amplitude of the current for each compound is omitted for clarity.

reaching up to 0.50 V. This is not unexpected for the Cu(II)/Cu(I) couple because of the considerable geometrical reorganization and charge balance involved in the process. A preferred tetrahedral geometry for the reduced ion is anticipated, and the presence of two phenolate ligands confer a negatively charged core. Because the $3d^{10}$ configuration of Cu(I) increases lability, one of the phenolate ligands might have its bond weakened or broken to decrease the electronic density around the metal.[6b,24,25] If metal reduction is prevented, one can focus on the most important features associated with the ligand-based processes. Two reversible or quasi-reversible processes are expected in these systems and associated with the oxidation of the *tert*-butyl phenolate species into the corresponding phenoxyl radicals. The radical nature of these species was also observed by spectrophotometric experiments, where addition of $(NH_4)_2[Ce^{IV}(NO_3)_6]$[26] to dichloromethane solutions of **3** and **3′** at room temperature yielded a new band respectively at 390 nm ($\varepsilon \sim 4500$ $L \cdot mol^{-1} \cdot cm^{-1}$) and 440 nm ($\varepsilon \sim 7000$ $L \cdot mol^{-1} \cdot cm^{-1}$) (Supporting Information Figure S1). The considerable difference in band position is in good agreement with previously reported values for copper-phenoxyl species conjugated to imine[27] and amine[28] groups and therefore similar to **3** and **3′**.

As can be seen in Figure 3, compound **1** shows limited reversibility with processes at 0.82 and 0.98 V vs Fc^+/Fc. The peak separation for the first process reaches 0.15 V and increases further to 0.16 V for the second process, rendering

(22) Aguilar-Martinez, M.; Saloma-Aguilar, R.; Macias-Ruvalcaba, N.; Cetina-Rosado, R.; Navarrete-Vazquez, A.; Gomez-Vidales, V.; Zentella-Dehesa, A.; Toscano, R. A.; Hernandez-Ortega, S.; Fernandez-G., J. M. *Dalton Trans.* **2001**, 2346.

(23) Elias, H.; Hasserodt-Taliaferro, C.; Hellriegel, L.; Schoenherr, W.; Wannowius, K. J. *Inorg. Chem.* **1985**, *24*, 3192.

(24) (a) Neves, A.; Rossi, L. M.; Bortoluzzi, A. J.; Szpoganicz, B.; Wiezbicki, C.; Schwingel, E.; Haase, W.; Ostrovsky, S. *Inorg. Chem.* **2002**, *41*, 1788. (b) Neves, A.; Verani, C. N.; de Brito, M. A.; Vencato, I.; Mangrich, A.; Oliva, G.; Souza, D. H. F.; Batista, A. *Inorg. Chim. Acta* **1999**, *290*, 207.

(25) Villeneuve, N. M.; Schroeder, R. R.; Ochrymowycz, L. A.; Rorabacher, D. B. *Inorg. Chem.* **1997**, *36*, 4475.

(26) Nair, V.; Deepthi, A. *Chem. Rev.* **2007**, *107*, 1862.

(27) (a) Parker, D.; Davies, E. S.; Wilson, C.; McMaster, J. *Inorg. Chim. Acta* **2007**, *360*, 203. (b) Benisvy, L.; Bill, E.; Blake, A. J.; Collison, D.; Davies, E. S.; Garner, C. D.; McArdle, G.; McInnes, E. J. L.; McMaster, J.; Ross, S. H. K.; Wilson, C. *Dalton Trans.* **2006**, 258.

(28) Halfen, J. A.; Jazdzewski, B. A.; Mahapatra, S.; Berreau, L. M.; Wilkinson, E. C.; Que, L., Jr.; Tolman, W. B. *J. Am. Chem. Soc.* **1997**, *119*, 8217.

them irreversible. The |Ipc/Ipa| peak ratio cannot be calculated accurately, but visual inspection suggests that the intensity of the anodic peak is greater than that of the cathodic peak indicating that |Ipc/Ipa| < 1. It implies that a smaller concentration of the phenolate species is present at the surface of the electrode in the time scale of the experiment because of either depletion or chemical transformation. Two well-shaped processes are observed for **3** at 0.53 and 0.83 V versus Fc^+/Fc. These seem to be quasi-reversible because ΔEp reaches 0.10 V at 100 $mV \cdot s^{-1}$, slightly larger than those values observed experimentally for the Fc^+/Fc couple under identical conditions. The quasi-reversibility is supported by an increase in the peak separation at higher scan rates with |Ipc/Ipa| values ranging from 1.27 at 100 $mV \cdot s^{-1}$ to 1.48 at 300 $mV \cdot s^{-1}$ for the first redox process. The insertion of bulky groups intended to enhance the amphiphilic properties in **4** appears to compromise the redox reversibility of the compound. The first ligand-centered peak is comparable to that of **3**, but a peak separation ΔEp of 0.14 V (|Ipc/Ipa| = 1.65), thus comparable to that of **1**, renders it irreversible. This irreversibility is increased in the second process. It is possible that the presence of tris(dodecyloxy)phenyl substituents increases the distance between the redox-active core of the molecule and the electrode surface, decreasing the rate of interfacial electron transfer, as seen in dendrimeric porphyrins.[29] From the point of view of redox reversibility, **3′** can be considered the best system. The ligand-centered processes shift to more positive potentials, namely 0.29 and 0.48 V versus Fc^+/Fc with separation peaks ΔEp = 0.09 V and |Ipc/Ipa| = 1.21, thus well within the limits observed for the Fc^+/Fc couple.

The switch-like activity is fundamental for potential uses in information storage and appears to depend heavily on the geometry adopted by the central atom. Octahedral systems tend to show rather limited switch-like cyclability, whereas five-coordinate systems[6] display reversible processes at 0.63 and 0.81 V vs Fc^+/Fc with minor decay after 20–50 cycles. To the best of our knowledge, the cyclability of square planar copper-phenolate systems is not known. On the basis of the data presented above, **3** and **3′** display good reversibility in the ligand-centered processes. Experiments were attempted cycling fifty times the two waves in a switch-like process. In spite of the initial results with **3**, a shift of up to 0.17 V can be detected between the first and the fiftieth cycle (Supporting Information Figure S2). The observed shift suggests a small but constant decay that might limit the use of this compound in responsive films. An excellent result was achieved with **3′** in which no significant changes (0.04 V) were detected after 50 cycles, thus indicating that decomposition of the generated species in the time scale of the voltammetry experiment did not take place. These results suggest that cycling of the phenoxyl species is viable in a flexible four-coordinate geometry and in noncoordinating solvents. Pending characterization of the amphiphilic properties of these two compounds, formation and study of Langmuir–Blodgett films of **3** and **3′** will be pursued.

(29) Pollak, K. W.; Leon, J. W.; Frechet, J. M. J.; Maskus, M.; Abruna, H. D. *Chem. Mater.* **1998**, *10*, 30.

Scheme 3

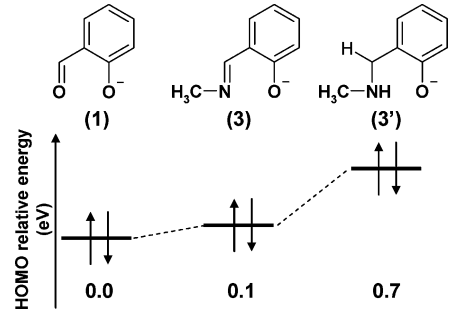

Electronic Structure Calculations. A series of computational calculations were run to correlate the experimental data observed for the ligand-centered redox properties of complexes **1**, **3**, **3′**, and **4** with their electronic nature. The B3LYP/6–311+G(d) level of theory[30] was employed to handle negatively charged species using the GAUSSIAN suite.[31] Geometries were fully minimized, without symmetry constraints, using standard methods.[32] It is assumed that all phenolate → phenoxyl processes described above will depend solely or mainly upon the relative energies of the HOMO orbitals of the ligand, from where electrons are withdrawn in an oxidative process, and that the higher the energy of the orbital, the more energetically affordable is the oxidation. Therefore, the models are nonmetallated and simplified versions of the deprotonated phenolate ligands as shown in Scheme 3. Considering that **1** shows the more positive potential, the HOMO orbital of the equivalent model system should be the lowest in energy and will display the lowest comparative energy. The model for **3** (also related to **4**) yields a higher comparative energy and that of **3′** exhibits the highest energy—therefore the most affordable oxidation process—in excellent agreement with the observed experimental trends. For **1** and **3**, π-delocalization seems to play an important role. One can conclude that energetically favorable oxidations can be achieved by replacing the —C═O by —C═NR groups attached to the phenolate ring. Similarly,

(30) (a) Becke, A. D. *Phys. Rev. A* **1988**, *38*, 3098. (b) Becke, A. D. *J. Chem. Phys.* **1993**, *98*, 5648. (c) Lee, T.; Yang, W. T.; Parr, R. G. *Phys. Rev. B* **1988**, *37*, 785. (d) Ditchfield, R.; Hehre, W. R.; Pople, J. A. *J. Chem. Phys.* **1971**, *54*, 724. (e) Gordon, M. S. *Chem. Phys. Lett.* **1980**, *76*, 163. (f) Hariharan, P. C.; Pople, J. A. *Theo. Chim. Acta.* **1973**, *28*, 213. (g) Hariharan, P. C.; Pople, J. A. *Mol. Phys.* **1974**, *27*, 209. (h) Hehre, W. R.; Ditchfield, R.; Pople, J. A. *J. Chem. Phys.* **1972**, *56*, 225.

(31) Frisch, M. J.; Trucks, G. W.; Schlegel, H. B.; Scuseria, G. E.; Robb, M. A.; Cheeseman, J. R.; Montgomery, J. A.; Vreven, T.; Kudin, K. N.; Burant, J. C.; Millam, J. M.; Iyengar, S. S.; Tomasi, J.; Barone, V.; Mennucci, B.; Cossi, M.; Scalmani, G.; Rega, N.; Petersson, G. A.; Nakatsuji, H.; Hada, M.; Ehara, M.; Toyota, K.; Fukuda, R.; Hasegawa, J.; Ishida, M.; Nakajima, T.; Honda, Y.; Kitao, O.; Nakai, H.; Klene, M.; Li, X.; Knox, J. E.; Hratchian, H. P.; Cross, J. B.; Bakken, V.; Adamo, C.; Jaramillo, J.; Gomperts, R.; Stratmann, R. E.; Yazyev, O.; Austin, A. J.; Cammi, R.; Pomelli, C.; Ochterski, J. W.; Ayala, P. Y.; Morokuma, K.; Voth, G. A.; Salvador, P.; Dannenberg, J. J.; Zakrzewski, V. G.; Dapprich, S.; Daniels, A. D.; Strain, M. C.; Farkas, O.; Malick, D. K.; Rabuck, A. D.; Raghavachari, K.; Foresman, J. B.; Ortiz, J. V.; Cui, Q.; Baboul, A. G.; Clifford, S.; Cioslowski, J.; Stefanov, B. B.; Liu, G.; Liashenko, A.; Piskorz, P.; Komaromi, I.; Martin, R. L.; Fox, D. J.; Keith, T.; Al-Laham, M. A.; Peng, C. Y.; Nanayakkara, A.; Challacombe, M.; Gill, P. M. W.; Johnson, B.; Chen, W.; Wong, M. W.; Gonzalez, C.; Pople, J. A. *GAUSSIAN 03*; Gaussian, Inc.: Wallingford, CT, 2003.

(32) Schlegel, H. B. *J. Comput. Chem.* **1982**, *3*, 214.

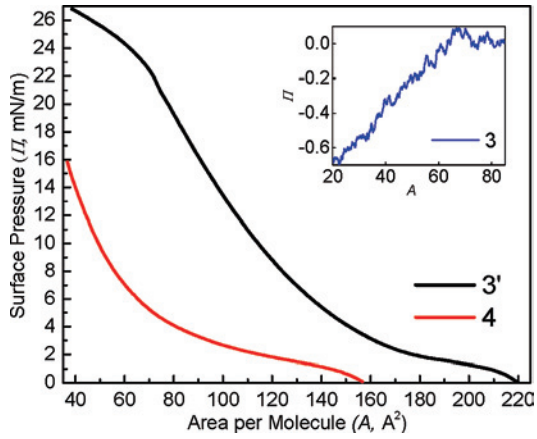

Figure 4. Compression isotherms for **3′** (black trace) and **4** (red trace).

it can be suggested that the nature of the group R attached to the Schiff base will have some impact in the electronic delocalization. This was observed for protonated models in which R = —CH_3 or —aryl, but the minimization of the deprotonated **4** seemed dependent on the orientation of that additional aryl ring. Interestingly, **3′** presents a localized π-frame limited to the aromatic phenolate ring. It can be concluded that disruption of the delocalization fosters energetically affordable oxidations and should be used as a guideline in the design of future amphiphilic precursors.

Amphiphilic Properties. The synthesis of **3** and **4** targets the attachment of nonpolar amine-containing organic fragments to the *tert*-butyl-containing precursor **1** by Schiff base condensation. These organic fragments have played an important role in the redox properties of these compounds and are expected to confer amphiphilic properties acting as hydrophobic counterparts of the copper-containing headgroup. In-situ reduction of **3** yielded **3′**. The amphiphilic properties of **3**, **3′**, and **4** were studied by means of compression isotherms plotting surface pressure (Π, mN/m) versus area per molecule (A, Å^2) and Brewster angle microscopy (BAM). The compression isotherms give information about the 2D behavior of the resulting Langmuir film at the air/water interface. The compression isotherms indicate the presence of mono or multilayers, collapse pressures, and average areas per molecule. BAM uses polarized light passing through media with dissimilar refractive indexes and is the most powerful method to identify structures such as agglomerates and domains in films at the air/water interface.

Recent studies on the C_{16}-containing copper surfactants described by Nagel et al.[13] have shown that longer octadecyl (C_{18}) chains tend to lead to an increase of collapse pressures.[33] Similarly, it has been demonstrated that replacement of the hydroxy groups by methoxy groups[34] yields complex behavior at the air/water interface. Therefore, considering the presence of bulky *tert*-butyl groups on **3**, longer octadecyl chains were employed. Nonetheless, the isotherm of **3** was marked by an erratic profile (Figure 4, inset) that confirms lack of organization and suggests random molecular aggregation. Loss of matter to the subphase was supported by areas as small as 15 Å^2·molecule^{-1} and pressures have no clear physical meaning. The presence of *tert*-butyl groups attached to the headgroup of **3** is key to the observed redox behavior of the compound but precludes the formation of organized films. Moreover, careful analysis of the disposition of the salicylaldehyde groups in **1**, as revealed by X-ray diffraction, suggests that the octadecylamine chains in **3** (and **4**) will be oriented trans to each other in a rigid imine-like structure. Exploratory BAM at several surface pressures distinctively shows the presence of oval-shaped domains (Supporting Information Figure S3) that resemble vesicles[1c,35,36] along with concentric domains, generally referred to as Newton rings.[37] These rings are multilayer granules formed from the ejection of matter from the compressed monolayer when localized oscillations are present. Thus, in addition to the headgroups, the rigidity of the framework appears to prevent this molecule from exhibiting amphiphilic properties.

Amphiphilic activity depends on an optimal balance between the hydrophobic and hydrophilic properties of a given surfactant. As such, ways of improvement were considered in the design of surfactants based on *tert*-butylsalicyl-copper head groups. Two possible approaches were examined, involving a decrease of the framework rigidity or an increase in the number of alkyl chains present. Imine reduction provided the amine surfactant **3′** with a more flexible framework, whereas **4** was used to increase the number of alkyl, or more formally alkoxy, chains present. Reduced **3′** was initially dissolved in dichloromethane and subsequently spread on the water surface. As the barriers of the trough were compressed, the tension (γ) of the air–water interface in the presence of the amphiphilic species decreased as compared to that of the bare air–water interface ($\gamma_0 = 72$ mN·m^{-1} at 23 °C), resulting in an increase in Π ($= \gamma_0 - \gamma$). Indeed, the isotherm (red trace) shown in Figure 4 exhibits considerable surface activity. Individual molecules begin interacting at very large areas of 220 Å^2, grow into a plateau-like region at low pressures, and increase consistently up to about 22 mN·m^{-1}, when an inflection takes place. The isotherm of **4** is also shown in Figure 4 and reveals this species as interfacially active. No inflections indicative of phase transitions are observed, and a moderate pressure of 14 mN·m^{-1} is reached.

Both approaches improve surface activity suggesting that a better equilibrium between hydrophilic and hydrophobic properties can be obtained in the design of redox-active surfactants. Interestingly, for both cases the compression barriers of the trough touch each other without the event of formal constant-area collapse characterized by a sudden decrease in the surface pressure.[38] We have suggested that metallosurfactants can exibit distinct collapse mechanisms,[14a]

(33) Pang, S.; Li, C.; Huang, J.; Liang, Y. *Colloids Surf.* **2001**, *A178*, 143.
(34) Hemakanthi, G.; Unni Nair, B.; Dhathathreyan, A. *Chem. Phys. Lett.* **2001**, *341*, 407.
(35) Dominguez-Gutierrez, D.; Surtchev, M.; Eiser, E.; Elsevier, C. J. *Nano Lett.* **2006**, *06*, 145.
(36) Svenson, S. *Curr. Opin. Colloid Interface Sci.* **2004**, *9*, 201.
(37) Galvan-Miyoshi, J.; Ramos, S.; Ruiz-Garcia, J.; Castillo, R. *J. Chem. Phys.* **2001**, *115*, 8178.
(38) (a) Vaknin, D.; Bu, W.; Satija, S. K.; Travesset, A. *Langmuir* **2007**, *23*, 1888. (b) Ybert, C.; Lu, W.; Moeller, G.; Knobler, C. M. *J. Phys.: Condens. Matter* **2002**, *14*, 4753.

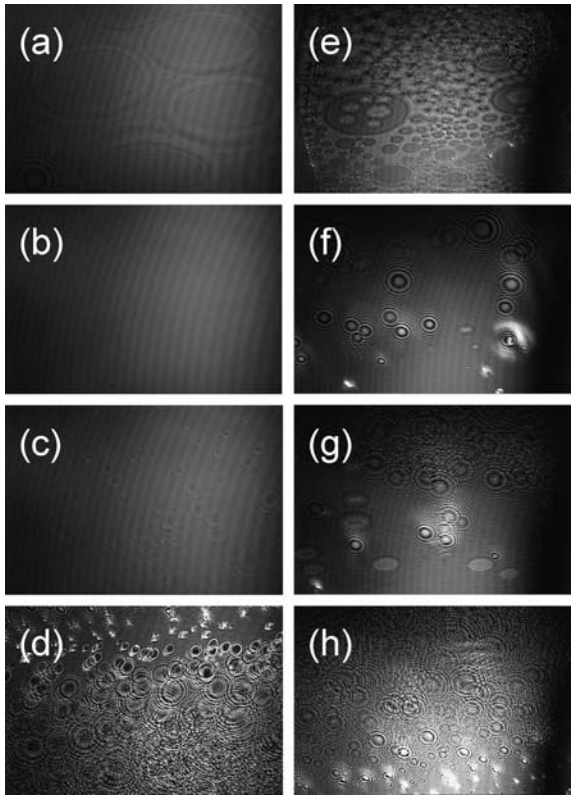

Figure 5. Brewster angle micrographs. For **3′:** (a) before compression, (b) below 2 $mN \cdot m^{-1}$, (c) at 6 $mN \cdot m^{-1}$, (d) at 21 $mN \cdot m^{-1}$. For **4**: (e) before compression, (f) at 3 $mN \cdot m^{-1}$, (g) at 5 $mN \cdot m^{-1}$, and (h) at 14 $mN \cdot m^{-1}$.

and this fact led to the consideration that, in spite of their shape, the isotherms describe the formation of multilayers. BAM was used to monitor the compression of **3′** and **4** in an attempt to investigate the nature of the resulting films. Figure 5 shows a series of selected micrographs gathered along the compression process for each of the amphiphiles.

Multiple domains are present before compression of **3′**. Before the first inflection in the isotherm, as well as at low surface pressures, an apparently homogeneous film is obtained. After this inflection the presence of Newton rings suggests instability of the film. At 20–21 $mN \cdot m^{-1}$ the film ceases to behave as a monolayer. Before compression of **4**, a film composed of several bidimensional oval-shaped domains is present. At about 3 $mN \cdot m^{-1}$ these domains seem to be replaced by a homogeneous monolayer, but the presence of several Newton rings suggest considerable instability. At 5 $mN \cdot m^{-1}$, rings and oval-shaped domains similar to those observed for **3** are present. Comparison of the domains present at 3 and 5 $mN \cdot m^{-1}$ suggest that only the former are flat, reinforcing the notion of a vesicular nature. Future dynamic light scattering experiments would be necessary to confirm this hypothesis. From 6 to 14 $mN \cdot m^{-1}$, a considerable increase in the roughness of the surface and the appearance of multiple rings takes place; this is interpreted as indicative of multilayers. Similar to the octadecyl chains, **4** has a rigid structure with trans-oriented trialkoxy groups. However, the three oxidodecyl ($-OC_{12}H_{26}$) chains present per amine can rotate almost freely. Contrary to **3**, these chains can point outward from the air/water interface, promoting a better equilibrium between the hydrophobic and hydrophilic portions of **4** and allowing for film formation. Because repulsion forces are also present, it is unlikely that all six chains can be aligned, accounting for the formation of multilayers.

Summary and Conclusions

In this Article we have used precursor **1** to develop a series of amphiphilic and redox-responsive complexes as candidates for the development of responsive films. We have demonstrated that the design of systems exhibiting a good balance between amphiphilicity and redox response is far from trivial. In **3** an apparent redox reversibility is obfuscated by a complete lack of amphiphilic behavior that prevents organization and ultimately the formation of films. The inclusion of three alkoxy groups per ligand in **4** appears to be key to the enhancement of the amphiphilic properties and to an improved response in the formation of relatively organized Langmuir films that show formal collapse at about 14 $mN \cdot m^{-1}$. Nonetheless, the redox-response was seriously compromised by an increased separation between cathodic and anodic peaks in the first phenolate/phenoxyl process. This behavior is a signature for a quasi-reversible process that is unlikely to withstand switch-like activities and is related to the nature and the bulkiness of the group attached to the imine function. Finally, an increased flexibility of the core was attained for **3′** by an in situ reduction of the C═N groups present in **3**. Improved amphiphilicity and consequent Langmuir film formation with a higher formal collapse at 27 $mN \cdot m^{-1}$ were observed. Moreover, excellent reversibility of the ligand-based processes and marginal decay upon switch-like cycling were also observed. The reversibility and cyclability seem to be associated with the disruption of the electronic delocalization between the phenolate and the C═N group and will be incorporated in the design of amphiphilic precursors for future responsive films.

On the basis of these results, it can be concluded that an increased flexibility of the core and electronic localization are fundamental to achieving a good balance between the desired redox and the amphiphilic properties. The replacement of the *tert*-butyl groups by other substituents that simultaneously foster phenolate/phenoxyl cycling and enhance the polarity of the headgroups—thus the amphiphilic behavior of the precursors—would be advantageous to the design of desired responsive Langmuir–Blodgett films. Recent advances[14b] suggest that chloro-groups might be able to deliver such properties. These results will pave the way to a new series of amine surfactants based on chloro-substituted phenolates coordinated to bivalent copper, nickel, and cadmium. The use of the latter cations should improve the thermodynamic stability of the resulting complexes leaving the ligand-centered redox activity unaltered. These topics are currently under development in our laboratories.

Experimental Section

Materials and Methods. All the reagents were obtained from commercial sources and were used without further purification. Dichloromethane was purified using an I.T. solvent purification

Table 1. Crystal Data for Complexes **1** and **5**[a]

complex	**1**	**5**
empirical formula	$C_{30}H_{42}Cu\ O_4$	$C_{32}H_{48}Cu_2\ O_6$
fw	530.18	655.78
temperature	100(2) K	100(2) K
wavelength	0.71073 Å	0.71073 Å
crystal system, space group	orthorhombic, *Pbca*	monoclinic, *C*2/c
unit cell dimensions	a = 7.8735(5) Å	a = 30.5691(9) Å
	b = 16.6446(11) Å	b = 9.5625(3) Å
	c = 20.9754(15) Å	c = 10.9862(3) Å
		β = 90.632(3) deg
volume	2748.9(3) Å^3	3211.26(16) Å^3
Z, calculated density	4, 1.281 Mg/m^3	4, 1.356 Mg/m^3
absorption coefficient	0.827 mm^{-1}	1.364 mm^{-1}
final R indices [$I > 2\sigma(I)$]	R1 = 0.0428,	R1 = 0.0506,
	wR2 = 0.1079	wR2 = 0.1254
R indices (all data)	R1 = 0.0764,	R1 = 0.0729,
	wR2 = 0.1201	wR2 = 0.1301

[a] $R(F) = \Sigma||F_o| - |F_c||/\Sigma|F_o|$; $wR(F) = [\Sigma w(F_o^2 - F_c^2)^2/\Sigma w(F_o^2)^2]^{1/2}$ for $I > 2\sigma(I)$.

system. IR spectra were measured from 4000 to 400 cm^{-1} as KBr pellets on a Tensor 27 FTIR-spectrophotometer. ESI spectra were measured on a Micromass QuattroLC triple quadrupole mass spectrometer with an electrospray/APCI source and Walters Alliance 2695 LC, autosampler and photodiode array UV detector. Experimental assignments were simulated based on peak position and isotopic distributions. Elemental analyses were performed by Midwest Microlab, Indianapolis, Indiana. UV–visible spectra of 1.0 × 10^{-4} M dichloromethane solutions were recorded in the range 200 to 1000 nm on a Cary 50 spectrophotometer. Electrochemical experiments were performed in dichloromethane on a BAS 50W voltammetric analyzer. A standard three-electrode-cell was employed with a glassy-carbon working electrode, a Pt-wire auxiliary electrode, and an Ag/AgCl reference electrode under an inert atmosphere at room temperature. $TBAPF_6$ was used as the supporting electrolyte. The |Ipa/Ipc| values were obtained using available software within the BAS package. All potentials are given versus Fc^+/Fc.[39]

X-ray Structural Determination for 1 and 5. Diffraction data were collected on a Bruker X8 APEX-II diffractometer equipped with Mo Kα radiation and a graphite monochromator at 100 K. Frames were collected at 10 s/frame (**1**) or 5 s/frame (**5**) and 0.3 degree between frames at a detector distance of 40 mm. The frame data were indexed and integrated with the manufacturer's SMART, SAINT, and SADABS software.[40] Both structures were refined and reported using Sheldrick's SHELX-97 software.[41] Crystals of **1** formed as brown plates and yielded 16135 reflections, of which 3652 were independent. Hydrogen atoms in **1** were placed in observed positions, and the asymmetric unit contains one-half complex with the Cu atom occupying an inversion center in the lattice. Crystals of **5** appeared as pale green plates, and 27592 reflections were harvested of which 3985 were independent. Hydrogen positions in **5** were observed or calculated. The asymmetric unit in **5** consists of one-half dimeric complex with the bridging methoxy groups occupying a 2-fold axis. The hydrogen atoms on these methoxy groups are disordered in two sets of partial positions.

Table 1 lists the experimental parameters.

Compression Isotherms. The $\Pi - A$ isotherms were measured in an automated KSV 2000 minitrough at 23 ± 0.5 °C. Ultrapure water (Barnstead NANO pure) was used for all experiments with a resistivity of 17.5–18 MΩ·cm^{-1}. Adventitious impurities at the surface of freshly poured aqueous subphases were removed by vacuum after barrier compression. Spreading of a known quantity (~30 μL) of 1.0 mg·mL^{-1} chloroform solutions on the aqueous subphase was followed by about 20 min equilibrium time before monolayer compression. The isotherms were obtained at a compression rate of 5 mm·min^{-1}. The pressure was measured using the Wilhelmy plate method (platinum plate, 40 mm perimeter). At least three independent measurements were carried out per sample with excellent reproducibility.

Brewster Angle Microscopy. A KSV-Optrel BAM 300 with a HeNe laser (10 mW, 632.8 nm) and a CCD detector was used in all micrographs. The compression rate was 5 mm/min, the field of view was 800 × 600 μm, and the lateral resolution was about 2 μm.

Syntheses. ***Caution!*** *Perchlorate salts are potentially explosive. Although the final products do not contain perchlorates, proper precautions should be taken for the synthesis.*

$[Cu(L^{SAL})_2]$ (1). Bis-(3,5-di-*tert*-butyl-2-phenolato-benzaldehyde)copper(II). To a stirring solution of 3,5-di-*tert*-butyl-2-hydroxy-benzaldehyde (0.515 g, 2.2 mmol) and 1.5 eq. triethylamine in 20 mL methanol was added a methanol solution (10 mL) of $Cu(ClO_4)_2 \cdot 6H_2O$ (0.375 g, 1 mmol), dropwise. After warming gently for 30 min, a brown microcrystalline solid was isolated by filtration. The precipitate was washed with 3 × 20 mL portions of cold methanol and 2 × 10 mL portions of cold ether and then dried under vacuum. The crude product was crystallized from 40 mL of methanol. After 24 h, a brown microcrystalline solid was isolated Yield = 95%. Anal. Calcd for $[C_{30}H_{42}O_4Cu]$: C, 67.96; H, 7.98. Found C, 67.77; H, 8.16%. IR (KBr, cm^{-1}) 1333 (υ_{C-O}), 1619 ($\upsilon_{C=O}$), 2868–957 (υ_{C-H} from *tert*-butyl groups). ESI pos. in MeOH: m/z = 530.1 for $[\mathbf{1} + H^+]^+$.

$[Cu^{II}(L^2)_2]$ (3). Bis-(2,4-di-*tert*-butyl-6-octadecyliminomethyl-phenolato)copper(II). To a stirring solution of octadecylamine (0.270 g, 1.0 mmol) in 20 mL ethanol was added the precursor **1** (0.265 g, 0.5 mmol) in 10 mL methanol, dropwise. The solution was refluxed for 1 h. The solvent was removed to obtain an olive colored powder. The power was dissolved in dichloromethane:methanol mixture (1:1) and yielded a homogeneous powder that was dried under vacuum overnight. Yield = 72%. Anal. Calcd for $[C_{66}H_{116}N_2O_2Cu]$: C, 76.72; H, 11.32; N, 2.71. Found C, 76.32; H, 11.44; N, 2.77%. IR (KBr, cm^{-1}) 1590 ($\upsilon_{C=N}$), 2859–2961 (υ_{C-H} from *tert*-butyl groups). ESI pos. in MeOH: m/z = 1033.2 for $[\mathbf{3} + H^+]^+$.

$[Cu^{II}(L^{2A})_2]$ (3′). Bis-(2,4-di-*tert*-butyl-6-octadecylaminomethyl-phenolato)copper(II). To a stirring solution of **3** (0.270 g, 1.0 mmol) in 20 mL of a 1:1 methanol:dichloromethane mixture at 0 °C small portions of $NaBH_4$ (0.12 g, 3.0 mmol) were added. The solution was kept in an ice bath until gas evolution ceased. The solvent was removed, and the crude product was dissolved in dichloromethane and washed with 10 × 100 mL aliquots of a saturated aqueous solution of sodium chloride. The resulting solution was dried on $NaSO_4$, and the dichloromethane evaporated to yield a pale green powder.

Yield = 60%. Anal. Calcd for $[C_{66}H_{120}N_2O_2Cu]$: C, 76.43, H, 11.66, N, 2.70. Found C, 76.63, H, 10.95, N, 2.68%. IR (KBr, cm^{-1}) 2860–2963 (υ_{C-H} from *tert*-butyl groups). ESI pos. in MeOH: m/z = 1036.9 for $[\mathbf{3'} + H^+]^+$.

$[Cu^{II}(L^3)_2]$ (4). Bis-(2,4-di-*tert*-butyl-6-[(3,4,5-tris-dodecyloxy-phenylimino)-methyl]-phenolato)copper(II). Precursor **1** (0.265 g, 0.5 mmol) was added to a stirring 20 mL methanol solution of 3,4,5-tris-dodecyloxy-phenylamine[42](0.646 g, 1.0 mmol) dropwise. After a mild reflux of 2 h, two-thirds of the solvent was removed to precipitate a brown powder. The powder was isolated and washed

(39) Gagne, R.; Koval, C.; Licenski, G. *Inorg. Chem.* **1980**, *19*, 2854.
(40) *APEX II, SMART, SAINT and SADABS collection and processing programs are distributed by the manufacturer.*; Bruker AXS Inc.: Madison, WI, U.S.A.
(41) Sheldrick, G. *SHELX-97*; University of Gottingen: Germany, 1997.

with cold methanol and dried under vacuum. Yield = 61%. Anal. Calcd for $[C_{114}H_{196}N_2O_8Cu]$: C, 76.65; H, 11.06; N, 1.57. Found C, 76.38; H, 11.16; N, 1.71%. IR (KBr, cm^{-1}) 1588 ($\upsilon_{C=N}$), 2852–2956 (υ_{C-H} from *tert*-butyl groups). ESI pos. in MeOH: m/z = 1784.9 for $[\mathbf{4} + H^+]^+$.

Acknowledgment. C.N.V. thankfully acknowledges the Wayne State University, the Donors of the ACS-Petroleum Research Fund (Grant 42575-G3), the Nano@Wayne initiative (Fund-11E420), and the National Science Foundation (Grant CHE-0718470), M.T.R. acknowledges the National Science Foundation (Grant CHE-0518262), and S.R.P.R. acknowledges the National Science Foundation (Grant CBET-0553537) for financial support.

(42) Percec, V.; Ahn, C.-H.; Bera, T. K.; Ungar, G.; Yeardley, D. J. P. *Chem.—Eur. J.* **1999**, *5*, 1070.

Supporting Information Available: Three figures and a table with data for compounds **1**, **3**, and **3′** (PDF). This material is available free of charge via the Internet at http://pubs.acs.org.

IC702233N